Journal of Hydroscience and Hydraulic Engineering
Vol. 11, No. 1, May, 1993, 41-50

TEMPERATURE STRUCTURES OBSERVED IN THE DESTRATIFICATION PROCESS IN A LAKE

By

Kenji Okubo

Disaster Prevention Research Institute, Kyoto University
Gokasho, Uji, Kyoto 611, Japan

SYNOPSIS

Temperature fluctuations due to interfacial waves were measured in a shallow lake within a frequency range between the internal wave with the maximum buoyancy frequency and the surface wind ripple. The interfacial waves were initiated by the amplified internal wave, and the wind waves transferred a similar structure to themselves on the density interface through the resonance mechanism with the generated interfacial waves to exhibit a definite inertial subrange in frequency spectra for temperature variations. Diffusivity took the peak at the lower bottom of the interfacial layer of linearly distributed temperature. For such profile of the diffusivity, the log+linear law for temperature profiles was retained, and parameters of the interfacial waves were estimated by fitting to a profile model. Calculating the interfacial waves as the form of cellular motions, structures of the interfacial waves were demonstrated and the calculated fluctuation was found to be similar to the variation of the measured temperature profiles.

INTRODUCTION

There is a wide variety of temperature variations in lakes ranging from the seiches to turbulence. In shallow lakes where diurnal destratifications occur quickly, some wavelike temperature variations could affect and disturb the mean temperature profile. In order to consider such structures, instantaneous water temperature profiles were measured every second for a duration of a few minutes. Such measurements were done several times during the typical destratification in a shallow lake. In the obtained records, temperature variations were significant within the intermediate frequency range between the internal waves and turbulent eddy motions. The components of which frequencies were higher than the maximum buoyancy frequency N corresponding to the steepest density gradient of the mean temperature profile, were termed as the interfacial waves to distinguish from ordinary internal waves, and their roles on mixing as roughness elements on the deformable density interface were discussed. In the following, time variation of the vertical structures of the water temperature, frequency spectra, internal wave dispersion and resonance mechanisms with the wind ripple, as well as the results from the profile model fitting and vertical eddy diffusivity analyses during the destratification are shown to reveal an overall organized structure accompanied by the cellular motions. Significance of those processes in surface layer dynamics was also discussed by Imberger and Patterson (4).

MEASUREMENTS USING THE THERMISTOR GRIDS

The measurements were carried out in North Lake in Perth, Western Australia. Its surface area is about 0.32 km^2 (mean diameter of 640 m) and the maximum depth is 2.4 m. The measurement station close to the lake heart was 1.9 m deep and a platform was built there. A thermistor bar contained 15 thermistors attached to it at intervals of 10 cm. Four bars were fit together in parallel with a spacing

of 20 cm and fixed up to form a plane grid. The four grids measured temperature at 240 points every second (or gridscan), which lasted for a few minutes in order to detect the structure of interfacial waves. The first grid was supported by rods and wires to be kept itself horizontal at a depth during a measurement and could be traversed only between the measurements. The other three grids were hung vertically with an equal spacing of 20 cm beneath the floor of the platform, each was placed between every two adjacent bars in the horizontal grid. As a result of the setting, the temperature records covered the upper 1.4 m within a horizontal area of 0.4 m by 0.6 m, with which the 12 vertical bars were enclosed.

Two quick response thermistors were attached to the horizontal grid with an electromagnetic current meter to get vertical velocity fluctuations, which allowed to estimate the heat flux at a depth. The gridscan consisted of channel scanning among the bars and layer switching with a selector. A 32 channels A/D conversion board was used with the 16-level selector to get 512 data within a gridscan. The cables for the switched outputs from the 16 thermistor bars were connected to the former 16 channels (with the selector) of the board and the inputs to the latter 16 channels (without selector) were signals from unswitched instruments such as the quick thermistors and the electromagnetic current meter. Further description about the measurement is found in Okubo (7).

In this paper, records on the day of a strong destratification, March 9, 1990 are shown, when the summer solar radiation made the lake water stratified in the morning. At local time 1049 (10:49) a weak, 2 m/s wind blew and ceased once at 1102 when the stratification became very stable. The sea breeze started to blow around 1133 and attained to 5 m/s, then blew at the constant speed after 1145, until the destratification was almost completed at 1224.

INTERNAL AND INTERFACIAL WAVES

Figure 1 shows the time variation of water temperature along the thermistor bar 11, close to the central vertical of the assembly and an initial temperature field of the destratification, which was taken in the measurement started at 1049. The vertical axis, z was taken downward from the water surface. Five isothermal patterns are cyclically used for every 0.2°C within a degree difference. Vertical interpolations were done after a temporal smoothing among every five successive profiles. Two values below the gray scale denote the maximum and the minimum temperatures observed (or interpolated) during the measurement. Temporal plots for the layers in the bar are also shown to accord each average temperature with its depth of measurement and the unit depth label (10 cm) with the amplitude of 1°C. A patch of warm water in the isothermal pattern should be found as a temperature rise in the time series.

Evolution of the destratification observed in the bar 11 is shown in Fig. 2. It was calm at 1102 and the 25°C isotherm at 15 cm depth below the water surface, the shallow interface, was somewhat wavy but of a smaller amplitude comparing with the other measurements before and after it; the 24°C isotherm at 40 cm depth corresponding to the lower bottom of the upper mixed layer was accompanied by billows of 20-30 cm amplitude. Patches of descending warmer and ascending colder water emerged alternately in the thicker lower layer. The 25°C isotherm began to break in the latter half of the record started at 1133 and after 1145 downwelling warmer water patches from the water surface became predominant in the records. At 1158, when the upper and the lower layers were of equal depths, magnitude of billows was smaller. The 24°C isotherm with billows, by which the destratification could be traced, existed at the 1.3 m depth by 1224. Throughout the day, the corresponding period to the maximum buoyancy frequency N was typically 70-100 seconds, while the apparent period of billows was 10-30 seconds, so the former was several times the latter. Thus, various waves cited in Turner (10) were seen between 0.01 Hz for N and 1 Hz, the sampling frequency of the gridscan.

The raw data of the quick thermistors were averaged within every second and the time series and their mean values are shown in Fig. 3; the records t_2 (dotted line) were taken at 2.5 cm above t_1 (solid line), and the same lines are used in the frequency spectra shown in Fig. 4, where in turn the raw data of the quick

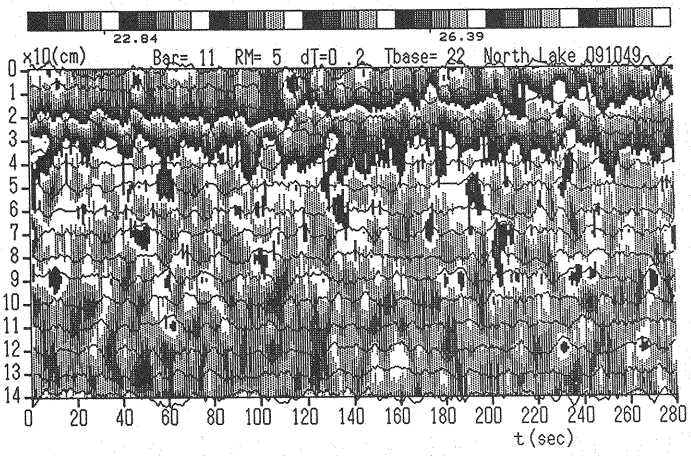

Fig. 1 Variation of temperature profiles and time series in each layer of the bar 11. The measurement started at 1049, March 9, 1990.

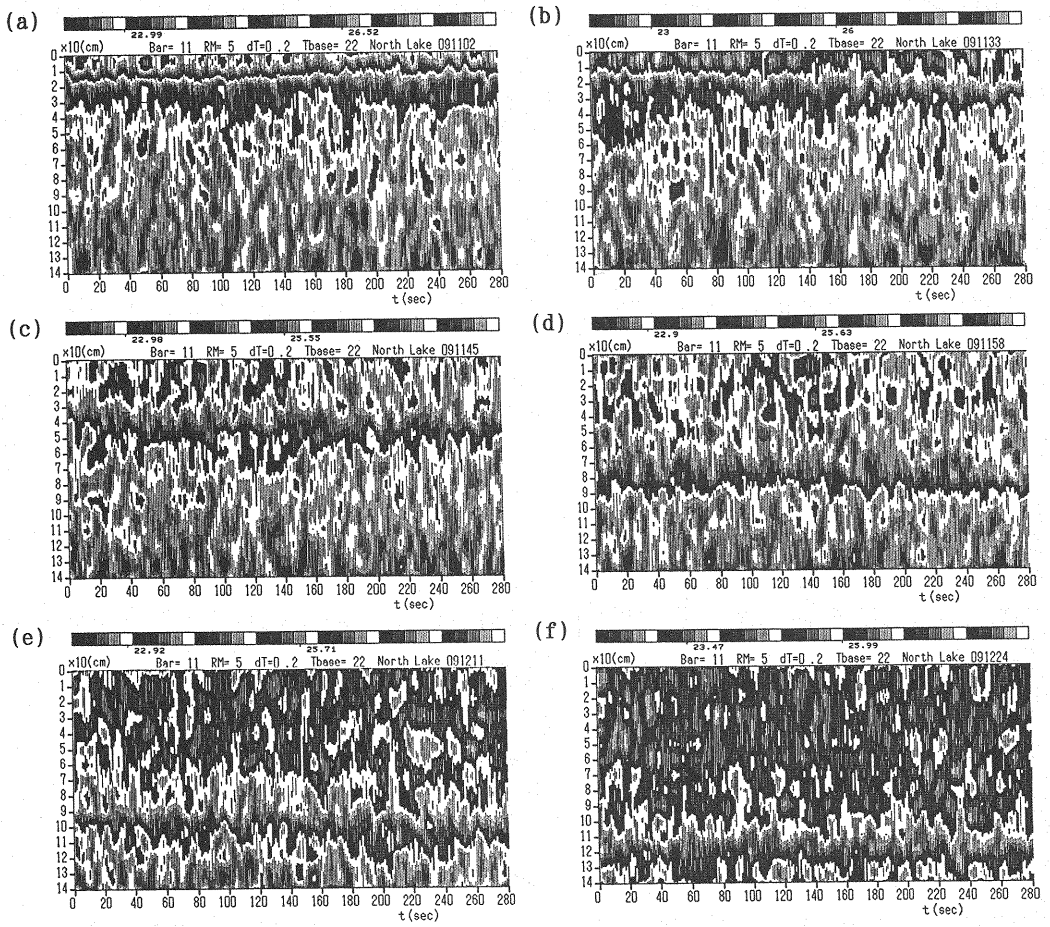

Fig. 2 Time-vertical structures in the bar 11 during the destratification started at (a)1102,(b)1133,(c)1145,(d)1158,(e)1211 and (f)1224 on March 9, 1990

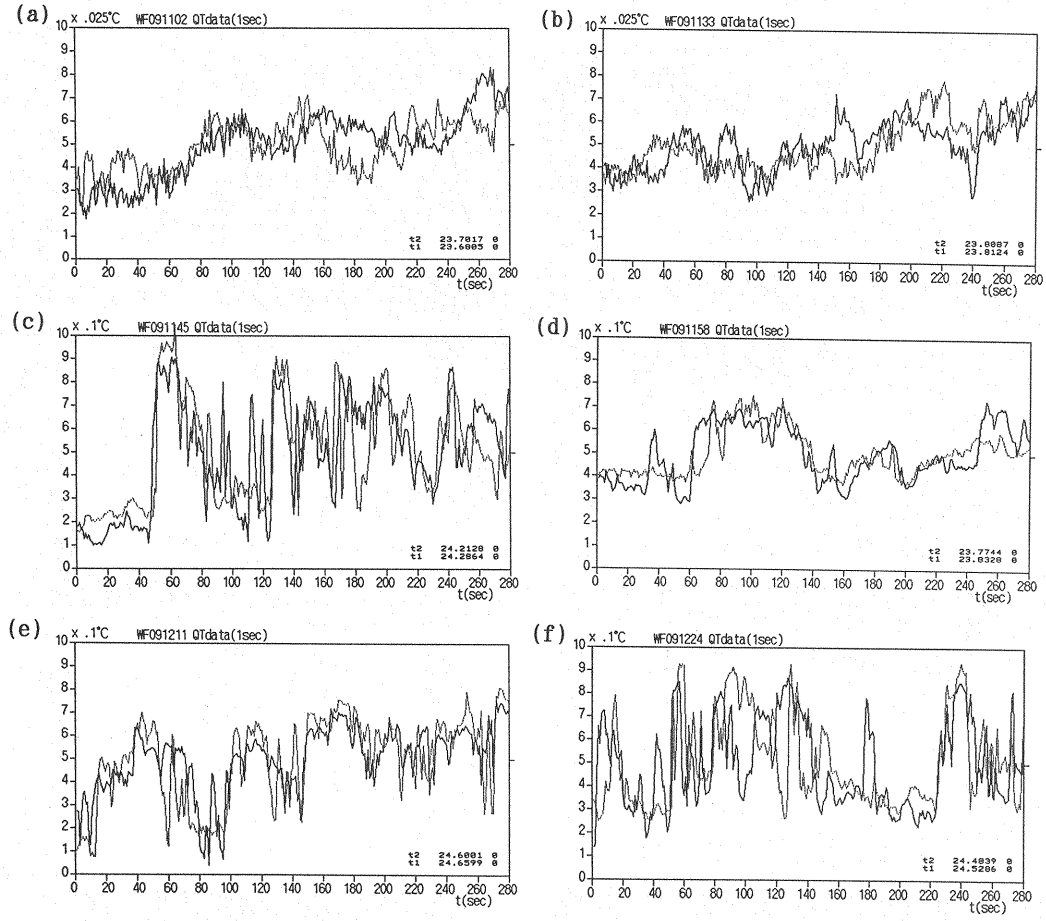

Fig. 3 Second averaged data of the quick response thermistors started at (a)1102,(b)1133,(c)1145,(d)1158,(e)1211 and (f)1224 on March 9, 1990

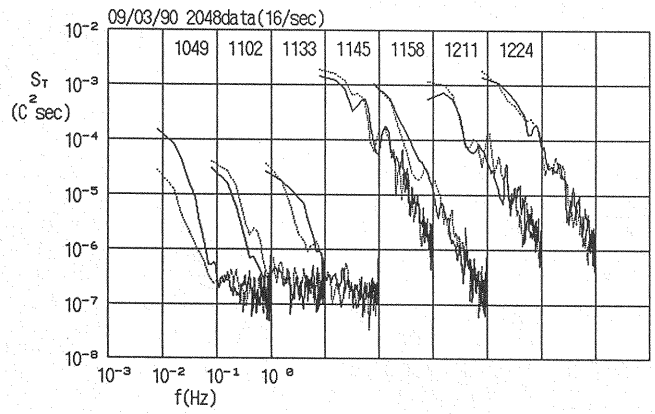

Fig. 4 Frequency spectra of temperature variations measured by the quick response thermistors (March 9, 1990)

thermistors were used for the spectral analyses. Their depths were changed from one measurement to another, according to the progress of the destratification. They were at 40-50 cm depth till 1155 and moved to the depths around 90 cm before 1158. Under the moderate wind, the temperature amplitude due to the internal wave was as small as 0.2°C, which was well described by the buoyancy frequency and the wave length of several meters. Larger variations of nearly 1°C magnitude occurred due to billows around 0.1 Hz, when the 24°C isotherm deepened and passed the depth of the thermistors.

FREQUENCY SPECTRA AND DISPERSION

Since 85 % of the time for a gridscan was spent to write the data on a file, data from the unswitched channels such as the quick thermistors were taken through a burst measurement with an active duration time ratio of 0.15, the sampling was intermittent. However, by regarding the raw records of the quick thermistors as 16 Hz sampling, the frequency, f spectra averaged for several bins of 2048 data were calculated and shown in Fig. 4. Because of the apparent peak at 1 Hz due to the gridscan, only the lower side of the spectrum is shown. At the calm stage, the spectral dependence on the frequency was f^{-1} on the higher side of 0.1 Hz and f^{-3} on the other side; the latter is similar to a buoyancy subrange. At the wind driven stage, an inertial subrange with the -5/3 power law became to be evident. Meanwhile, when the lake was in a weak and continuous stratification, the viscous-convective subrange with the -1 power law was observed as well as under calm conditions. Thus, aspects of wave number spectra in deep oceans discussed by Monin and Ozmidov (5) were also found in frequency spectra in a shallow lake.

The inertial subrange due to the wind was clearly observed and that it was within the frequency range of the interfacial waves. It would be explained that the cascade down process could be interpreted as a self deforming process of the internal wave, on condition that the frequency modulation of the finite amplitude internal wave was dominant. Figure 5 shows the dispersion relationships reviewed by Turner (10) for internal waves under the lake condition of the day. Regarding the interfacial waves as the higher terms of the finite amplitude basic internal wave, (N,k_N) and assuming the j-th resonant waves (jN,jk_N), shown as solid circles in Fig. 5, are generated as algebraic sum for both the angular frequency ω and the wave number k. Dispersion relationships by Hunt (3) and Thorpe (9) for a shallow upper layer (h_1), represents the generation of the interfacial waves, where the amplitude of the internal wave, a was assumed to be 0.3 m. Another resonance process with the wind ripple at the water surface seems possible and would follow.

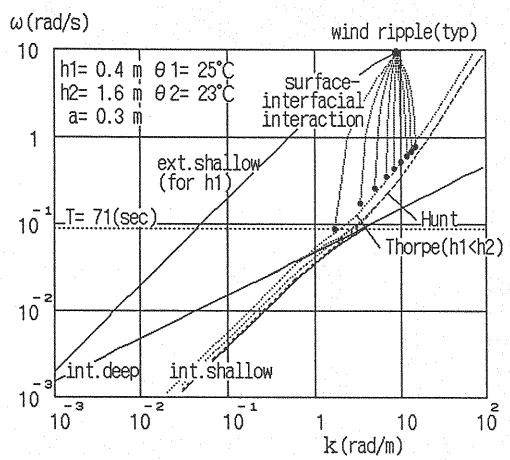

Fig. 5 Dispersion relationships for the internal waves, resonant interfacial waves and the surface-interfacial interaction

The wave number of the wind ripple is in the range of the interfacial waves, however, the frequency is much higher than jN, so resonances between the interfacial waves and the wind ripple (noted as surface-interfacial interaction in the figure) could be effective to generate higher resonant waves close to the characteristics of the wind ripple in the ω-k domain. Thus, when the amplitude of the internal wave, a, increases subject to the shallow water dispersion, the internal waves are covered with the shorter interfacial waves and the interface is highly roughened, which would result in wind mixing.

MEAN PROFILES AND VERTICAL EDDY DIFFUSIVITY

The mean density profiles by spatial (among the vertical bars) and a temporal averaging for each layer temperature are shown in Fig. 6. These profiles can be divided into three parts; a constant, linear and logarithmic parts and these are conjugated at the upper and the lower bottoms of the intermediate linear layer, $z=z_b$ and z_a, respectively. The heat fluxes were estimated from time change rates of the heat content storaged in the water column between successive temperature profiles. Net radiation was estimated from photo sensor outputs and the radiative flux was assumed to be distributed for the entire depth with the attenuation coefficient of 2.1 m^{-1}. The heat flux was converted into temperature flux, and the diffusivity profiles, K(z) were estimated in Fig. 7. The diffusivity ranged 1 to

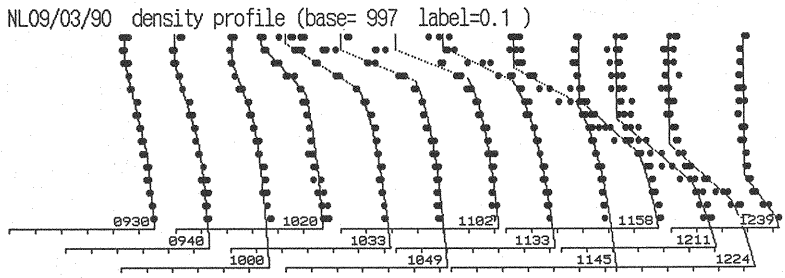

1/ 090930	3/ 091000	5/ 091033	7/ 091102	9/ 091145	11/ 091211	13/ 091239
6.9697	5.64103	8.78049	10	5.41667	4.94949	3.23232
4.44946E-03	0.00439	3.76077E-03	2.75484E-03	4.33774E-03	5.84389E-03	6.70949E-03
2.00202E-07	2.44052E-07	4.86902E-07	3.02371E-07	7.53406E-07	1.34222E-06	9.76433E-07
0.69	0.44	0.36	0.22	0.26	0.49	0.32
0.099	0.078	0.041	0.022	0.048	0.099	0.099
1.5942	1.9697	0.758621	0.785714	1.04167	0.758621	2.41667
0.09	0.09	0.150126	0.127273	0.177231	0.266327	0.128017

2/ 090940	4/ 091020	6/ 091049	8/ 091133	10/ 091158	12/ 091224
5.85859	5.21127	10.9091	7.22222	4.88095	4.34343
5.14747E-03	6.15236E-03	2.75484E-03	3.27492E-03	6.18033E-03	5.70953E-03
3.09977E-07	7.86744E-07	2.87072E-07	4.79932E-07	1.14162E-06	1.2367E-06
0.58	0.37	0.24	0.26	0.41	0.43
0.099	0.071	0.022	0.036	0.084	0.099
1.89655	2	0.758621	0.703704	1.26087	0.875
0.09	0.0959459	0.120833	0.196761	0.162489	0.263123

Fig. 6 The fitted density profiles to the measured density data shown as full circles and the estimated parameters (March 9, 1990)

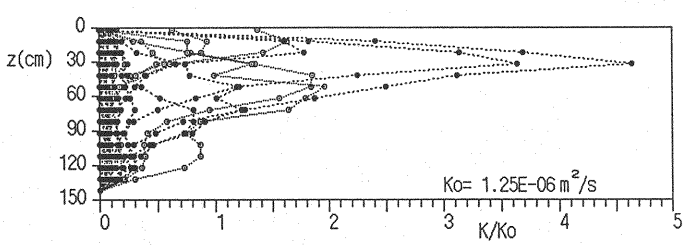

Fig. 7 Profiles of the eddy diffusivity; open and full circles denote the diffusivities on March 8 and 9, 1990, respectively

5 times the kinematic viscosity K_0 at the mean temperature. The maximum K appears below the interface, while in deeper part, temperature gradient was so small that calculated K sometimes took unreasonably large values. To avoid this, K was set to be zero there and estimated only for the gradients larger than 0.02°C/m.

Using the interfacial friction velocity u_*, diffusion to viscosity ratio β, von Karman constant κ, and a factor η, K(z) may be expressed as

$$K(z)=\beta\kappa u_* z \exp(-\eta z) \tag{1}$$

The above equation has been applied to meteorological and oceanographic cases as reviewed by Henderson-Sellers (2) and noticed in another shallow lake by Okubo and Muramoto (6). In the upper mixed layer, that is especially thin in shallow lakes, diffusivities are small and some convective motions as well as radiations maintain the inverse layer near the water surface instead of diffusion.

Consider a frequency relationship, $\omega_1>\omega_2>\omega_1-\omega_2(\omega_1<2\omega_2)$, where ω_1 and ω_2 are the local buoyancy frequencies corresponding to the maximum density gradient near the interface ($\omega_1=N$) and a milder one in the lower layer, respectively. Since the wave velocity ω/k is constant in shallow water dispersion relationships, which is valid during a destratification, hence $k_1>k_2>k_1-k_2$. Thus, the internal wave with the wave length of $2\pi/(k_1-k_2)$ would be generated at the lower bottom of the linear layer. With the corresponding length δ (the choice is arbitrary as it is eliminated) and the dimensionless depth, $\zeta=\eta z$, Eq. 1 is rewritten as

$$\delta=(\beta/\eta)\zeta\exp(-\zeta) \tag{2}$$

With the temperature flux $u_*\theta_*=\kappa u_*\delta(d\theta/dz)$ and Eq. 2,

$$\theta/\theta_*=(\beta\kappa)^{-1}\left[\ln\zeta+\gamma+\sum_{n=1}^{\infty}\{(\zeta^n/n!)/n\}\right]_{\zeta_0}^{\zeta}$$

is retained. Taking the term only for n=1, the above is a log+linear law for the temperature profile with a roughness parameter ζ_0 as

$$\theta/\theta_*=(\beta\kappa)^{-1}\{\ln(\zeta/\zeta_0)+(\zeta-\zeta_0)\} \tag{3}$$

With the interfacial wave height, a, in place of η^{-1}, Eq. 1 is rewritten as

$$K(z)=\beta\kappa u_* z \exp(-z/a) \tag{4}$$

Thus, active mixing due to the maximum eddy observed as billow is expected at the depth of peak diffusivity, namely at the bottom of the linear layer, $\zeta=z/a=1$. The length δ in Eq. 2 is interpreted as the maximum wave length due to the resonance between the basic internal waves in the linear and the logarithmic layers.

The log+linear profile is expected in the shallow lake. In present case, a length-based profile model is preferable to flux-based original profile. It is a formal wall law, in which kinematic viscosity is replaced by a constant eddy viscosity $\kappa u_* s$ in the linear layer with a lateral spacing of interfacial waves, s. When the upper mixed layer is formed, $\zeta=z'/a$ is defined as for $z'=z-z_b$. Figure 6 shows model parameters for each profile, which are record time; $\lambda=a/s$=wave slope; u_*; $B=g'w_e$=buoyancy flux; $a=z_a-z_b$=thickness of the linear layer, which is identified with the interfacial wave height; s=lateral wave spacing; β=inverse Prandtl number; and $\chi=\lambda^{-1}\beta^{-1}=w_e/\beta\kappa u_*=g'a/(u'_a)^2$=Richardson number in the linear layer, where w_e and $u'_a=u_a-u_b$ are the vertical flux velocity scale and the shear scale between z_a and z_b. The profile of the density excess $\rho'=\rho-\rho_0$ is

$$\rho'/\rho'_a=(\beta+\zeta)/(\beta+1) \qquad 0<\zeta<1 \tag{5a}$$

$$=1+\chi\ln\zeta \qquad \zeta>1 \tag{5b}$$

$$\rho_0=(1+\beta)\rho_a-\beta\rho_b \tag{6}$$

and ρ_a, ρ_b are the densities at $z=z_a$ and z_b, by which the density difference is defined as $\Delta\rho=\rho_a-\rho_b$, and $g'=(\Delta\rho/\rho_0)g$ with the gravity acceleration g. In the fitting process, s was found to be around 0.1 m, less than δ, typically a quarter the interfacial wave height a, and $\lambda=4$ was tried first. The reference density, $\rho_0=997$ kg/m^3 was used instead of Eq. 6, while χ was estimated using λ and $\beta=(\rho'_a/\rho'_b-1)^{-1}$. If the χ value was less than a minimum of 0.09, it was replaced by the minimum (an outline is shown in Okubo (7)). Then $u_*=\kappa(\beta g's)^{1/2}$ [m/s] and $B=g'\chi\beta\kappa u_*$ [m^2/s^3] were caluculated.

Laboratory experiments by Faller and Caponi (1) on the Langmuir circulation shows that a pair of longitudinal cells exists in a diagonal of wind ripple, which means the cell radius is a quarter the lateral wave length. Thus, it was strongly suggested that the similar cell structure existed in the linear layer, by which the wind ripples would copy their structure on the interface.

CELLULAR MOTION

Consider the ray wave in stratified fluids, where the interfacial wave could be extracted as the cellular motion (Prandtl (8), Turner (10)) in the crosswind vertical plane. Because of the higher frequency than N, the interfacial waves are not strictly on the analytic basis for the linear internal wave. Whilst thinking of incomplete wave characteristics of the interfacial waves, it is more likely for them to cause mixing. With the buoyancy frequency $(g'/a)^{1/2}$ in the linear layer, which corresponds well to the density profile, $\rho=\rho_s\exp(z/H)$, two constituents of the interfacial waves, of which frequencies are 2 to 6 times higher than the basic internal wave (j=2, 3 and 6), are assumed to exist through the whole depth. From the condition of the measurements, the basic period was the same as in Fig. 5. Instantaneous cellular motions are shown in Fig. 8. The periods are 35, 23 and 11 seconds, which accord with the measured ones. The wave length of the mode, j=6

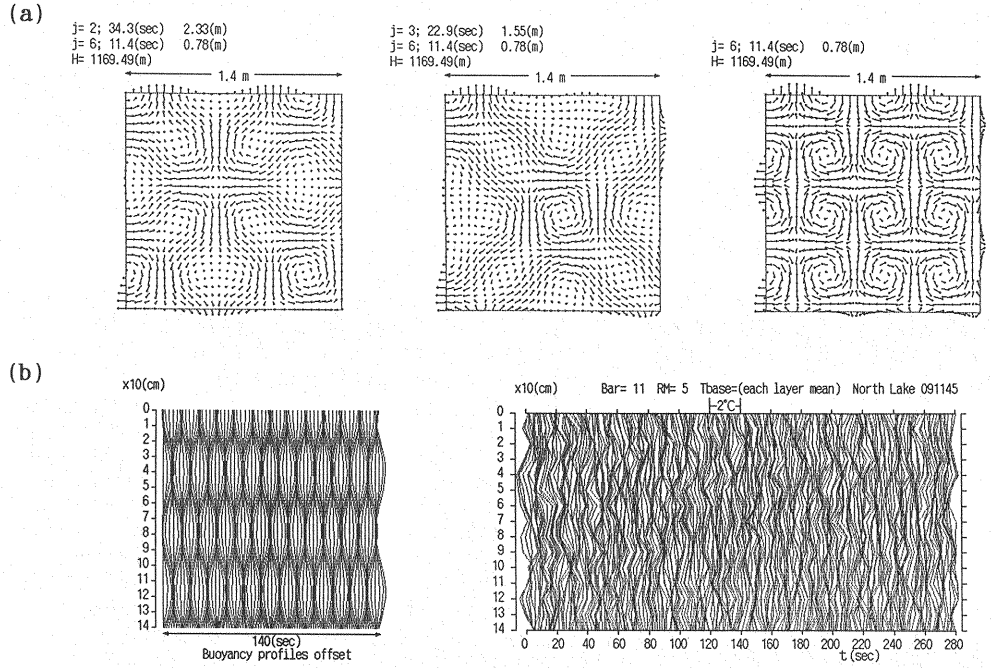

Fig. 8 Cellular motion; (a) calculated instantaneous vector fields (b) calculated variation of buoyancy profiles; and the measured variation of the profiles of temperature deviation from each layer mean in the bar 11, started at 1145 on March 9, 1990

with the period of 11 seconds was 0.78 m, which means a cell size of about 40 cm. In Fig. 8(b), variation of the buoyancy profiles and the measured variation of the profiles of the temperature deviation from the time averaged values in the layers. They show similar temporal patterns, however, because of other quicker interfacial waves and slower internal wave, apparent nodal depths are not clear in the field (see also Fig. 1). Strong billows do not occur near the interface in calculations since an uniform buoyancy frequency was assumed. However, the interfacial waves of several times higher than the buoyancy frequency were dominant and a layered cell structure in the crosswind section was shown.

CONCLUSION

From spectral analyses of temperature fluctuation during the destratification in the shallow lake, an definite inertial subrange was obtained in the frequency band between the minimum internal wave and the interfacial waves. The interfacial waves, which are generated through an internal process as the frequency modulation of the finite amplitude internal wave, interact with wind ripples of the surface mode and acquire the similar configuration to the wind ripples, while the energy of surface waves seems to be transferred into the internal mode. An internal wave with the wave length inversely proportional to the difference of the wave numbers between the upper and the lower layers, works as a continuous source of billows. The estimated profile of the diffusivity shows a peak at the lower bottom of the linear layer and decays within a distance of the wave height, a, and active mixing is confined to the billowing layer. In such diffusive field, the log+linear law was expected and verified using the profile model. The results for the density excess were demonstrated, where the interfacial waves were found to be important as the roughness elements on the deformable density interface. Cell structures relating to the lateral spacing of the interfacial waves (or the wind ripples) was considered in the cross wind vertical plane, and fluctuation of buoyancy profile due to the cellular motion was compared with the measured one. Periods of the dominant interfacial waves were well explained by the calculation, and multi layer cellular structures were extracted.

The author thanks to Prof. Jörg Imberger and the staffs in the Centre for Water Research, the University of Western Australia, for their advises and technical supports to arrange the measurement. Financial supports for field trips and the data processing were indebted from Centre for Environmental Fluid Dynamics, UWA, and also from the Scientific Research Fund (grant for Prof. Akira Murota, Osaka Commercial University) by the Ministry of Education, Science and Culture.

REFERENCES

1. Faller, A.J. and E.A. Caponi : Laboratory experiments of wind driven Langmuir circulation, J. Geophys. Res., Vol.83, No.C7, pp.3617-3633, 1978.
2. Henderson-Sellers, B. : Engineering Limnology, Monographs and Surveys in Water Resources Engineering, 8, Pitman, pp.75-93, 1984.
3. Hunt, J.N. : Interfacial waves of finite amplitude, La Houille Blanche, 16, pp.515-531, 1961.
4. Imberger, J. and J.C. Patterson : Physical Limnology, Advances in Applied Mechanics, Vol.27, Academic Press, pp.334-353, 1990.
5. Monin, A.S. and R.V. Ozmidov : Turbulence in the Ocean, Environmental Fluid Mechanics, Reidel, pp.146-151, 1985.
6. Okubo, K. and Y. Muramoto : Vertical water diffusivity of wind-driven currents in a shallow lake, Proc. 6th Cong., APD, IAHR, Vol.III, pp.193-200, 1988.
7. Okubo, K. : Measurements of Destratification in a shallow lake using the thermistor grids, Annuals, Disast. Prev. Res. Inst., Kyoto Univ., No.34B-2, pp.319-336, 1991 (in Japanese).
8. Prandtl, L.: Essentials of fluid dynamics, London, Blackie, p.240, 1952.
9. Thorpe, S.A.: On the shape of progressive internal waves, Phil. Trans. Roy. Soc. London, A, 263, pp.563-614, 1968.
10. Turner, J.S.: Buoyancy effects in fluids, Cambridge Univ. Press, 1973.

APPENDIX - NOTATION

The following symbols are used in this paper:

- a = interfacial wave height or thickness of the linear layer;
- B = buoyancy flux;
- f = frequency;
- g, g' = gravity and reduced gravity;
- h_1, h_2 = upper and lower layer depths;
- H = imaginary depth of the exponential density profile;
- j = integer for the higher modes;
- k, k_1, k_2 = wave numbers;
- k_N = wave number of the basic internal wave;
- K, K_o = vertical eddy diffusivity and kinematic viscosity;
- δ = maximum billow size;
- N = maximum buoyancy frequency;
- s = lateral spacing of the interfacial waves;
- S_T = spectrum for the temperature variation;
- t = elapsed time in a mesurement;
- t_1, t_2 = the temperatures measured by the quick thermistors;
- u_* = shear velocity at the interface;
- u'_a = velocity shear within the linear layer;
- w_e = vertical velocity scale of the vertical flux;
- z = vertical coordinate;
- z_a, z_b = depth of the lower and upper bottom of the linear layer;
- γ = an integral constant;
- $\Delta\rho$ = density difference;
- λ = slope of the interfacial wave;
- ρ = density of water;
- ρ_o = reference density;
- ρ_a, ρ_b, ρ_s = density at $z=z_a$, z_b and water surface;
- ρ' = density excess;
- θ = temperature;
- θ_1, θ_2, θ_* = upper, lower and friction temperatures;
- χ = Richardson number;
- η = inverse length scale;
- ζ, ζ_o = dimensionless depth and roughness; and
- ω, ω_1, ω_2 = angular frequencies.

(Received November 20, 1992; revised April 15, 1993)